EUROPEAN ORGANIZATION FOR NUCLEAR RESEARCH

Status report to the ISOLDE and Neutron Time-of-Flight Committee

(Following HIE-ISOLDE Letter of Intent I-111)

2^+ Anomaly and Configuration Isospin Polarization of ^{136}Te

September 24, 2019

R. Zidarova[1], G. Rainovski[2], N. Pietralla[1], V. Werner[1], P. John[1], R. Kern[1], P. Koseoglou[1], T. Kröll[1], P. Napiralla[1], J. Wiederhold[1]

[1]*Institut fur Kernphysik, Technische Universitat Darmstadt, 64289 Darmstadt, Germany*
[2]*Faculty of Physics, St. Kliment Ohridski University of Sofia, 1164 Sofia, Bulgaria*

Spokesperson: R. Zidarova (rzidarova@ikp.tu-darmstadt.de)
Co-Spokespersons: N. Pietralla (pietralla@ikp.tu-darmstadt.de)
G. Rainovski (rig@phys.uni-sofia.bg)

CERN-INTC-2019-022 / INTC-SR-079
24/09/2019

Abstract:

It is proposed to perform a Coulomb excitation experiment on ^{136}Te. The ^{136}Te radioactive ion beam will be delivered by HIE-ISOLDE with an energy of 5.0 MeV/u impinging on a ^{208}Pb target. The γ-rays of deexcitation will be detected by the MINIBALL array and scattered particles will be detected by a Double Sided Silicon Strip Detector (DSSSD) in forward direction. The Configurational Isospin Polarization of the two lowest-lying 2^+ states will be determined by measuring the $E2$ excitation yield distributed to them. Furthermore, the emergence of collectivity and the nucleon-nucleon interactions will be investigated by populating the yrast 4^+ and 6^+ states.
The supposed mixed-symmetry character of the 2^+_2 and 2^+_3 states will be tested. Complementary lifetime information on predominant 2^+_2 state will be extracted using the differential DSAM technique.

Requested shifts: 12 shifts
Installation: MINIBALL + CD-only

1 Introduction

The impact of local shell structure on the proton-neutron (pn) balance of low-energy 2^+ states at the onset of collectivity near neutron rich shell closure is of particular interest for contemporary nuclear research. Two fundamental one-phonon quadrupole excitations are normally found in near-spherical nuclei, both mixtures of the underlying proton and neutron 2^+ configurations. They can be simplified into a two-state mixing scenario $\left|2_i^+\right\rangle = \alpha_i \left|2_\pi^+\right\rangle \pm \beta_i \left|2_\nu^+\right\rangle$. The 2^+ state, resulting from an in-phase combination of proton and neutron contributions, is the fully symmetric state (FSS). The other one is the pn-mixed-symmetry state [1] with the opposite phase - the lowest energy isovector valence shell quadrupole excitation. Mixed-symmetry states (MSS) can be experimentally identified by their strong isovector $M1$ decay to the low-lying fully-symmetric states [2]. MSSs are a unique ground for investigating the balance between nuclear collectivity [3, 4], shell structure [2, 5] and isospin degrees of freedom.
The absolute $B(M1; 2_{ms}^+ \rightarrow 2^+)$ strength probes the relative pn contributions in the wave function. A mechanism called Configurational Isospin Polarization (CIP) occurs when proton and neutron amplitudes in the one-phonon 2^+ state wave functions are not balanced, and either one dominates. This effect may occur near shell closures with neutron excess, such as ^{90}Zr and ^{132}Sn [6, 7]. Significant CIP was found to manifest in a reduction of absolute $M1$ rates between the two one-phonon 2^+ states and a simultaneous increase of $E2$ excitation strength of the 2^+ state with dominant proton contribution. A while ago, CIP was held responsible [8, 9] for the occurrence of the 2^+ anomaly observed in ^{136}Te [10]. More recently, results from high-energy Coulomb excitation experiments [11, 12] presented new values on the $B(E2; 0_1^+ \rightarrow 2_1^+)$, which are not in agreement with previous findings. This suggests that the wave function of the 2_1^+ is dominated by excited valence neutron configurations, but not to the extend previously suggested. However, $B(E2)$ strengths for both states and the $M1$ strength between them are needed in order to uniquely quantify the amount of CIP.

2 Physics case

For nuclei only a few particles away from closed shells, one can apply the seniority scheme in order to describe the low-lying excited states. Those states are formed by recoupling of angular momenta of unpaired nucleons. Multiplets of states with the same number of unpaired nucleons are formed. This number is called *seniority* - ν [13]. In even-even nuclei the seniority scheme [14, 15] is represented in a few experimentally measurable ways [16, 17]:

- excited yrast states follow an energy pattern such like the j^2 configuration
- absolute $B(E2)$ strengths for seniority changing transitions follow a parabolic scheme of increase with the filling of j-shell and reach maximum in its middle
- absolute $B(E2)$ strengths for seniority conserving transitions follow a parabolic scheme of increase with the filling of j-shell and reach minimum in its middle

When the number of valence nucleons increases, proton-neutron interaction becomes more prominent [21] and collectivity emerges. The process of transition from single-particle to collective behaviour in nuclei is yet unclear. Evolution of quadrupole collectivity is tested against four experimental criteria:

- energy of the first excited 2_1^+ state $E(2_1^+)$
- ratio $R_{4/2} = E(4_1^+)/E(2_1^+)$
- absolute transition strength $B(E2; 2_1^+ \rightarrow 0_1^+)$
- ratio $B_{4/2} = B(E2; 4_1^+ \rightarrow 2_1^+)/B(E2; 2_1^+ \rightarrow 0_1^+)$

Even though values for these parameters are strictly defined only for a few special cases, in most cases the set of criteria can serve well for discrimination against collective and non-collective character in nuclei.
The ^{136}Te isotope has two valence protons and two valence neutrons outside the doubly-magic core of ^{132}Sn. This simple system provides a convenient frame for exploring the emergence of collectivity and nucleon-nucleon interactions. Moreover, with the increase of the neutron excess, dramatic changes in nuclear properties may be observed. The structure of the first excited levels of ^{136}Te can be described as a superposition of the excitations in its two even-even neighbours - ^{134}Te and ^{134}Sn, as presented at Fig. 1. Those neighbouring nuclei have both 2 same type particles outside doubly-magic core and they exhibit strong seniority-like regime. The question, which emerges, is whether seniority is still a good quantum number in ^{136}Te. Collectivity should be tested using the criteria, listed above, and by measuring the absolute transition strength $B(M1; 2_2^+ \rightarrow 2_1^+)$ and by determining the extent, to which CIP is is presented in the wave function of 2_1^+ and 2_2+ excited states.
The energy of the first 2_1^+ state in ^{136}Te is relatively low, which indicates that the $\nu f_{7/2}$ part of the wave function is stronger than the $\pi g_{7/2}$ part, since the neutron pair breaks more easily than the proton pair. This can be supported by simple calculations using the three point formula for the binding energy [18]. Thus the wave function of the 2_1^+ state has a large component of neutron excitation. Complementary is the fact of a similar behaviour of nuclei near the doubly magic core of ^{208}Pb [19].

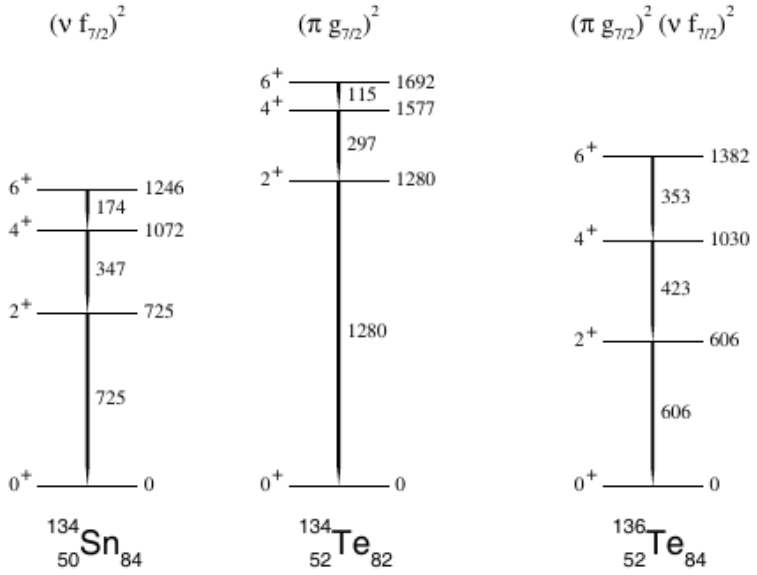

Figure 1: Partial level scheme of ^{134}Te, ^{134}Sn and ^{136}Te. First excited states in ^{134}Te and ^{134}Sn are result of residual interaction in a two-particle configuration - $(\nu f_{7/2})^2$ and $(\pi g_{7/2})^2$ respectively. Structure of first levels in ^{136}Te is superposition of the excitations in its neighbours. Image taken from Ref. [19]

Experimental results support neutron dominance in the 2_1^+ state . First studies of this isotope [10] indicate reduction of the $B(E2; 2_1^+ \rightarrow 0_1^+)$ transition probability with respect to lighter isotopes. This smaller value clearly violates the empirical rules for properties of quadrupole collective states [20, 21]. This unusual behaviour is considered "the 2^+ anomaly of ^{136}Te". The significant lowering of the $B(E2; 2_1^+ \rightarrow 0_1^+)$ value in ^{136}Te in comparison with ^{132}Te implies considerably different structures of the wave functions of these isotopes. This would suggest, as proposed above, neutron dominated character of the 2_1^+ state [22, 23, 26]. The availability of two proton orbitals - $1g_{7/2}$ and $2d_{5/2}$ would lead to proton dominated 2_2^+ state, which may lead to a significant $B(M1; 2_2^+ \rightarrow 2_1^+)$ transition strength and a large $B(E2; 0_1^+ \rightarrow 2_2^+)$ excitation strength from the ground state. Measurements of these observables are needed to understand better the structure of these excited states. Furthermore, the study would be extended to higher-lying states - namely the 4_1^+ and 6_1^+ states, in order to determine their composition and follow the gradual manifestation of nuclear collectivity.
More recent studies of ^{136}Te [11, 12], including high-energy Coulomb excitation reactions, show an enhanced reduced transition probability than previously measured. The new values are not consistent with previous measurements and imply prolate-deformed quadrupole collectivity and greater proton content than expected. There are examples in literature about discrepancies between results from Coulomb Excitation experiments and other methods that allow direct lifetime measurements, such as Doppler effect based methods. An example for that is given in Ref. [24, 25] Therefore, a new measurement of the 2_1^+ lifetime of ^{136}Te is of highest interest. Moreover, the transition strength $B(E2; 4_1^+ \rightarrow 2_1^+)$ and upper limits for the $B(E2; 2_2^+ \rightarrow 2_1^+)$ and $B(E2; 2_2^+ \rightarrow 0_1^+)$ transition strengths have been measured in both experiments. Summery of all measured values is presented in

Table 1: Comparison of the experimental values for transition probabilities $B(E2; I_i \rightarrow I_f), [e^2b^2]$ of ^{136}Te

$0_1^+ \rightarrow 2_1^+$	$2_2^+ \rightarrow 0_1^+$	$2_2^+ \rightarrow 2_1^+$	$4_1^+ \rightarrow 2_1^+$	Reference
0.122(18)				Danchev et al. [8]
0.122(24)				Fraile et al. [28]
0.191(26)			0.061(31)	Vaquero et el. [12]
0.181(15)	<0.004	<0.09	0.060(9)	Allmond et al. [11]

Table 1. As a conclusion of those there is no enhanced $E2$ excitation probability of the 2_2^+ state and the experimental results are in agreement with Shell Model calculations [26, 27]. However, more experimental data are needed to further clarify this point, since there is a lack $B(M1)$ transition strengths, which are the most characteristic feature of mixed-symmetry states. Thus, we propose an experiment using projectile Coulomb excitation of the nucleus ^{136}Te produced by ISOLDE using the MINIBALL spectrometer in conjunction with the standard DSSSD (CD detector) and, simultaneously, a variant of the Doppler Shift Attenuation Method (DSAM) for extraction of lifetimes.

3 Feasibility of the proposed experiment

We propose a combined experiment using the well-established technique of sub-barrier projectile Coulomb excitation to extract the electromagnetic matrix elements of transitions between excited states in ^{136}Te and, simultaneously, a variant of the Doppler Shift Attenuation Method for extraction of the lifetimes of short-lived states of ^{136}Te projectile nuclei.

The ^{136}Te ions will be produced by ISOLDE with a standard UCx /graphite target. ^{136}Te ions can be extracted with intensities $> 4 \cdot 10^7$ ions/μC from the UCx/graphite target [30]. They will be charge-bred by REX-EBIS and accelerated by the HIE-ISOLDE to energies of 680 MeV (5 MeV/u). A considerable contamination of the beam with isobaric ions, in particular ^{136}Xe, may persist after charge-breeding. Therefore we request to use a selective laser-ionization scheme by means of RILIS and intend to measure in the well-kown laser on/off-mode. Laser schemes have been successfully tested with Ti:Sa lasers [29]. Additionally, in an effort to suppress surface-ionized isobaric contaminants the Laser Ion Source and Trap (LIST) will be used [31]. Application of LIST will affect the production of Te and reduce it by a factor of 20-50. A beam intensity of $\approx 10^4 - 10^5$ ions/s can be expected at the secondary target of 2.5 mg/cm^2 of ^{208}Pb at MINIBALL. Both projectile and target nuclei will be excited via Coulomb excitation in the scattering process. The scattered nuclei will be detected by the annular CD detector placed 20 mm behind the secondary target and covering scattering angles of 24-62 degrees in the laboratory system. The reaction kinematics is shown in Fig. 2. Scattered target-like and beam-like nuclei will be detected in the DSSSD. The energy of the projectile ions has been chosen such that safe Coulomb excitation is ensured for all scattering angles covered by the DSSSD. Deexcitation γ-rays will be detected by the MINIBALL array. Background will be suppressed by employing particle-gamma coincidences.

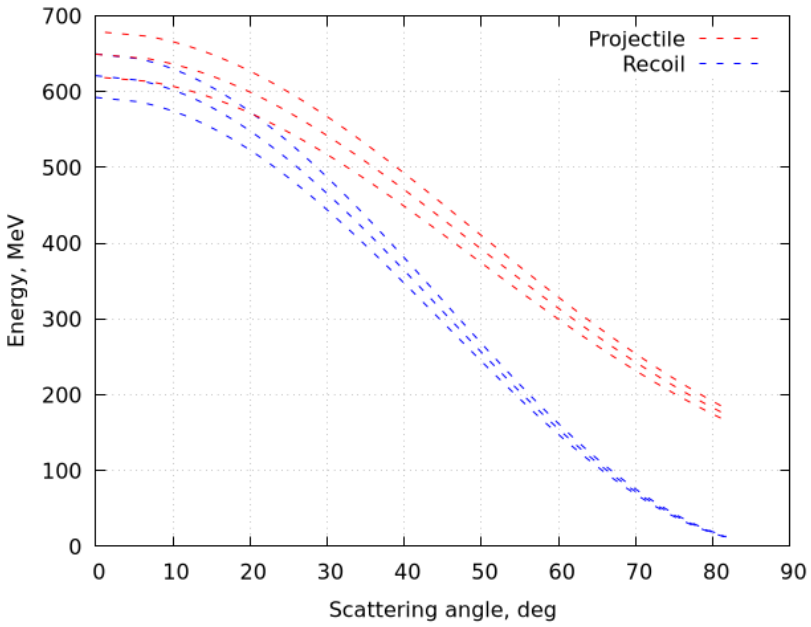

Figure 2: Kinematics plot for ^{136}Te at 5 MeV/u impinging on a 2.5 mg/cm^2 ^{208}Pb. Kinematics are shown for beam energy at entrance, middle and exit of target.

The electromagnetic matrix elements for the transitions of the projectile nucleus ^{136}Te will be extracted from a fit of the matrix elements to the experimentally observed γ-ray yields. A normalization can be performed using the known value for $B(E2; 2_1^+ \rightarrow 0_1^+)$. Complementary lifetime information on the short-lived states of ^{136}Te will be extracted using the differential DSAM [32] technique. This type of analysis is already well-established for stopped ion beams and can be adopted for in-flight γ-ray emission, i.e. without stopping the beam in the target. The method is based on the velocity-dependent Doppler shift of γ-rays emitted by ions in flight.
Nuclei that are excited to very short-lived states have a considerable probability of decaying before their passage through the target material is completed – in contrast to long-lived states, which are most likely to decay when the projectile ions are already behind the target. In the latter case, the velocity distribution of the emitting nuclei for a given scattering angle is very sharp – close to a delta function, leading to a sharp peak after applying the Doppler correction for the ion velocities behind the target. On the contrary, γ-rays from fast decays are emitted at varying velocities with a well-defined distribution depending on the stopping power of the target material, the target thickness and the level-lifetime. Because the individual ion velocities at the time of de-excitation are not directly accessible, the known ion velocities behind the target have to be assumed in the Doppler-correction. This results in a characteristic line shape in the Doppler-corrected γ-ray spectrum, comparable to the line shape of the well-known DSAM measurements using stopped beams, although less strongly pronounced. In the analysis of the data, the computer code APCAD [33] will be used to calculate the velocity distribution of the ions and to perform a fit of the lifetime to the observed angular-dependent line shapes in the γ-ray spectra. To ensure a significant lifetime-effect on the line shape, the passage-time of the projectiles through the target has to be on the same order of magnitude as the

Table 2: Estimated cross sections and count rates for projectile Coulomb excitation of ^{136}Te on a 2.5 mg/cm^2 lead target. γ-ray detection efficiency is assumed to be 5%. Beam intensity is 10^5 pps

Level	Energy, keV	Cross section, mb	Yield (cts/day)
2_1^+	606	$2{,}23.10^3$	6900
4_1^+	1030	$5{,}67.10^1$	176
2_2^+	1568	$2{,}03.10^1$	64

lifetime of the emitting state. The 2_2^+ state is an ideal candidate to be investigated using this method. Due to the large $M1$ transition to the 2_1^+ state, it is expected to decay after a lifetime of $\approx$ 100 fs. This number is also predicted by the recent calculations of Ref. [9]. In addition, we intend to analyze the γ-ray angular distribution of the decay of the 2_1^+ (and if possible 2_2^+) states in order to perform a RIV analysis to extract absolute magnetic moments that will sensitively test the neutron character of the 2_1^+ state.
Estimates for the expected count rates have been calculated using the standard Coulomb Excitation code CLX and presented in Table 2. Recent results for reduced transition strengths [11] have been used for the calculations. Energy loss in the target has been taken into consideration when calculating the cross-sections. The interaction is assumed to happen in the middle of the target. The total efficiency for γ-ray detection of MINIBALL is estimated to be 5%.
In order to achieve sufficient statistical accuracy in the Coulomb excitation analysis, three days of beam on target are requested to collect the data for the de-excitation of the high-spin states - 4_1^+ and 6_1^+, and the $2_2^+ \rightarrow 2_1^+$ transition. Additionally, one day for testing the beam composition with the LIST target is required. The beam composition will be determined by using the ionization chamber and observation of decay radiation with MINIBALL.

4 Summary

Summary of requested shifts: 12 shifts in total - 3 shifts (one day) for testing of beam production and composition and 9 shifts (three days) for CE yield measurement in laser on/off mode

References

[1] F. Iachello, Phys. Rev. Lett. **53**, 1427 (1984)

[2] N. Pietralla et al., Prog. Part. Nucl. Phys. **60**, 225 (2008)

[3] K. Heyde and J. Sau, Phys. Rev. C **33**, 1050 (1986)

[4] T. Ahn et al., Phys. Lett. B **679**, 19 (2009)

[5] G. Rainovski et al., Phys. Rev. Lett. **96**, 122501 (2006)

[6] J. D. Holt et al., Phys. Rev. C **76**, 034325 (2007)

[7] V. Werner et al., Phys. Rev. C **78**, 031301 (2008)

[8] M. Danchev et al., Phys. Rev. C **84**, 061306 (2011)

[9] A. P. Severyukhin et al., Phys. Rev. C **90**, 011306 (2014)

[10] D. C. Radford et al., Phys. Rev. Lett. **88**, 222501 (2002)

[11] J. M. Allmond et al., Phys. Rev. Lett. **118**, 092503 (2017)

[12] V. Vaquero et al., Phys. Rev. C **99**, 034306 (2019)

[13] A. de Shalit, I. Talmi, Nuclear Shell Theory (Academic Press, New York) (1963)

[14] I. Talmi, Nucl. Phys. A **172**, 1 (1971)

[15] I. Talmi, Simple Models of Complex Nuclei, (Harwood Academic Press, Switzerland) (1993)

[16] J. J. Ressler et al., Phys. Rev. C **69**, 034317 (2017)

[17] R. F. Casten, Nuclear Structure from a Simple Perspective (Oxford University Press, NewYork) (2000)

[18] W. Satula, J. Dobaczewski, W. Nazarewicz, Phys. Rev. Lett. **81**, 3599 (1998).

[19] A. Astier et al., Eur. Phys. Jour. A **46**, 165-185 (2010)

[20] L. Grodzins, Phys. Lett. **2**, 88 (1962)

[21] R. F. Casten, Nucl.Phys. A **443**, 1 (1985)

[22] J. Terasaki et al., Phys. Rev. C **66**, 054313 (2002)

[23] N. Shimizu et el., Phys. Rev. C **70**, 054313 (2004)

[24] J. M. Allmond et al., Phys. Rev. C **92**, 041303(R) (2015)

[25] A. Jungclaus et al., Phys. Lett. B **695**, 110 (2011)

[26] A. Covello et al., Prog. Part. Nucl. Phys. **59**, 401 (2007)

[27] V. Vaquero Soto, Ph.D thesis, Universidad Autonoma de Madrid, 2018

[28] L.M.Fraile et al., *Proceedings of the 23th International Nuclear Physics Conference* (2008)

[29] RILIS databse, URL: http://riliselements.web.cern.ch/riliselements/

[30] ISOLDE yield information, URL: https://oraweb.cern.ch/pls/isolde/query tgt

[31] D. A. Fink et al., Nucl. Instr. and Meth. in Phys. Res. B **317**, 417-421 (2013)

[32] C. Stahl, PhD Thesis, TU-Darmstadt (2015)

[33] C. Stahl et al., Comp. Phys. Comm. **214**, 174-198 (2017)

Appendix

DESCRIPTION OF THE PROPOSED EXPERIMENT

The experimental setup comprises: MINIBALL + CD only, Ionization Chamber

Part of the	Availability	Design and manufacturing
MINIBALL + only CD	☒ Existing	☒ To be used without any modification
Ionization chamber measurement	☒ Existing	☒ To be used without any modification ☐ To be modified
	☐ New	☐ Standard equipment supplied by a manufacturer ☐ CERN/collaboration responsible for the design and/or manufacturing
Implantation and Decay Study	☒ Existing	☒ To be used without any modification ☐ To be modified
	☐ New	☐ Standard equipment supplied by a manufacturer ☐ CERN/collaboration responsible for the design and/or manufacturing

HAZARDS GENERATED BY THE EXPERIMENT (if using fixed installation:) Hazards named in the document relevant for the fixed MINIBALL + only CD + Ionization Chamber installation.

Additional hazards:

Hazards	MINIBALL + CD only	Ionization Chamber measurement	Implantation and decay study
Thermodynamic and fluidic			
Pressure			
Vacuum			
Temperature			
Heat transfer			
Thermal properties of materials			
Cryogenic fluid			
Electrical and electromagnetic			
Electricity			
Static electricity			
Magnetic field			
Batteries	☐		
Capacitors	☐		
Ionizing radiation			
Target material	^{208}Pb, stable	No target	^{197}Au or similarly heavy, stable

Beam particle type (e, p, ions, etc)	ions (^{136}Te)	ions (^{136}Te)	ions (^{136}Te)
Beam intensity	maximum available (below 10^7 /s	maximum available (below 10^7 /s	maximum available (below 10^7 /s
Beam energy	680 MeV	680 MeV	680 MeV
Cooling liquids			
Gases			
Calibration sources:	☒		
• Open source	☒^{241}Am/ Triple-Alpha		
• Sealed source	☒^{60}Co,^{152} Eu		
• Isotope			
• Activity			
Use of activated material:			
• Description	☐		
• Dose rate on contact and in 10 cm distance			
• Isotope			
• Activity			
Non-ionizing radiation			
Laser			
UV light			
Microwaves (300MHz-30 GHz)			
Radiofrequency (1-300 MHz)			
Chemical			
Toxic			
Harmful			
CMR (carcinogens, mutagens and substances toxic to reproduction)			
Corrosive			
Irritant			
Flammable			
Oxidizing			
Explosiveness			
Asphyxiant			
Dangerous for the environment			
Mechanical			
Physical impact or mechanical energy (moving parts)			

Mechanical properties (Sharp, rough, slippery)			
Vibration			
Vehicles and Means of Transport			
Noise			
Frequency			
Intensity			
Physical			
Confined spaces			
High workplaces			
Access to high workplaces			
Obstructions in passageways			
Manual handling			
Poor ergonomics			

Hazard identification:

Average electrical power requirements (excluding fixed ISOLDE-installation mentioned above): 0 kW